#### RESEARCH



# Self-Organized Criticality in a Relativistic Yukawa Theory with Luttinger Fermions

Holger Gies<sup>1,2,3</sup> · Marta Picciau<sup>1</sup>

Received: 27 June 2025 / Accepted: 29 August 2025 © The Author(s) 2025

#### Abstract

We propose and investigate a Yukawa model featuring a dynamical scalar field coupled to relativistic Luttinger fermions. Using the functional renormalization group (RG) as well as large- $N_{\rm f}$  or perturbative expansions, we observe the emergence of an infrared attractive partial fixed point in all interactions at which all couplings become RG irrelevant. At the partial fixed point, the scalar mass parameter is RG marginal, featuring a slow logarithmic running towards the regime of spontaneous symmetry breaking. The long-range behavior of the model is characterized by mass gap formation in the scalar and the fermionic sector independently of the initial conditions. Most importantly, a large scale separation between the low-energy scales and the microscopic scales, e.g., a high-energy cutoff scale, is naturally obtained for generic initial conditions without the need for any fine-tuning. We interpret the properties of our model as a relativistic version of self-organized criticality, a phenomenon observed in specific statistical or dynamical systems. This entails natural scale separation and universal long-range observables. We determine nonperturbative estimates for the latter including the scalar and fermionic mass gaps.

## 1 Introduction

Quantum field theories with scalar fields are prototypical for theories with phase transitions, since the potential of the scalar field can trigger different realizations of the ground state depending on its location and possible symmetry-breaking features in field space. Already at zero temperature, phase transitions can occur as a function of the parameters of the models,

 Holger Gies holger.gies@uni-jena.de
 Marta Picciau marta.picciau@uni-jena.de

Published online: 10 October 2025

- Theoretisch-Physikalisches Institut, Abbe Center of Photonics, Friedrich Schiller University Jena, Max Wien Platz 1, 07743 Jena, Germany
- Helmholtz-Institut Jena, Fröbelstieg 3, D-07743 Jena, Germany
- <sup>3</sup> GSI Helmholtzzentrum für Schwerionenforschung, Planckstr. 1, 64291 Darmstadt, Germany



specifically the parameters and couplings entailed in the scalar potential. The underlying mechanisms find application in a wide range of fields from statistical mechanics, condensed matter physics to elementary particle physics and cosmology.

The parameter region near a phase transition typically features critical phenomena and is often governed by fluctuations of the scalar fields, potentially giving rise to features of universality [1]. In relativistic four-dimensional spacetimes, approaching the critical region generically requires a fine-tuning of parameters. This is because the mass parameter of the scalar field represents a relevant direction of the renormalization group (RG) with a power-counting exponent near two; the latter implies that microscopic parameters of a model have to be tuned with quadratic precision to certain values in order to observe near-critical features in the long-range physics.

A prominent example for such properties is the Higgs sector of the standard model of particle physics where the mass of the Higgs boson characterizing the low-energy scale is much smaller than anticipated high-energy scales such as those of grand-unified theories or the Planck scale of gravity. The correspondingly anticipated necessity of fine-tuning of parameters, specifically the scalar mass parameter, is often considered as unnatural. Solutions to this naturalness problem [2–5], or rather explanations for the seemingly specific parameter choices, have inspired a large number of suggestions for new underlying particle physics models.

Standard suggestions involve, for instance, a removal of the relevant direction by postulating an additional symmetry (e.g., scale, conformal, or supersymmetry) or by replacing the fundamental scalar by an alternative or composite degree of freedom that becomes effective near the electroweak scale (e.g., technicolor, little Higgs models, etc.).

In the present work, we explore a different option which is well known in the context of dynamical systems: if a system has a critical point that is an attractor of the evolution the macroscopic properties can display critical phenomena without the need to tune microscopic parameters to specific values. This *self-organized criticality* [6] can, for instance, be observed in slowly driven nonequilibrium many-body systems with nonlinear dynamics [7–11]. Translated into relativistic quantum field theory, where the transition across scales, i.e., RG time, plays the role of time in nonequilibrium systems, this requires an interacting scalar model with a slow (e.g., logarithmic) RG running near a suitably infrared (IR) attractive fixed point. This is clearly at odds with the strongly relevant mass parameter of a scalar model near the standard Gaussian fixed point.

A possible scenario for self-organized criticality in a relativistic theory has first been sketched by Bornholdt and Wetterich in [12] where the necessary critical point has been suggested to occur in the form of a partial RG fixed point for the running scalar-field expectation value to be stabilized by a sufficiently large scalar anomalous dimension. It has been argued in [12] that this stabilization could occur for a suitable matter content.

In our work, we show that a partial infrared attractive RG fixed point occurs naturally in Yukawa theories with scalar fields interacting with relativistic Luttinger fermions. The latter have recently been proposed as novel particle degrees of freedom giving rise to new asymptotically free field theories [13]; the relativistic version generalizes Luttinger fermions [14] known from various non-relativistic condensed-matter systems, e.g, with electronic excitations near quadratic band touching points [15–21]. The partial fixed point occurs in our model for the Yukawa coupling as well as for all scalar self-interactions rendering all these



couplings RG irrelevant. At the same time, the partial fixed point goes along with a large scalar anomalous dimension which renders the scalar mass parameter RG marginal. In the course of the RG flow, the latter exhibits a slow logarithmic drift towards the transition from the symmetric to the broken regime. Once the transition occurs, the partial fixed points are destroyed and the system settles in the broken phase with a gapped spectrum. No fine-tuning is needed for a scale separation of the low-energy observables from the microscopic scales — in direct analogy to self-organized criticality in dynamical systems.

We define our Yukawa model in Section 2. For the analysis of the model, we utilize the functional RG as detailed in Section 3. A leading-order analysis, including large- $N_{\rm f}$  or perturbative methods is presented in Section 4. A nonperturbative analysis using a local potential approximation of the functional RG is performed in Section 5, where also first quantitative estimates for the low-energy observables are computed. The high-energy completion of the Yukawa model in terms of an asymptotically free fixed point of a purely fermionic model is discussed in Section 6. We conclude in Section 7. Some technical details are described in the appendices.

## 2 The $\gamma_{11}$ Yukawa Model

Our model is inspired by a purely fermionic model of self-interacting relativistic Luttinger fermions first discussed and analyzed in [22]. The classical Euclidean action of this model reads

$$S_{\rm F} = \int d^4x \left[ -\bar{\psi} G_{\mu\nu} \partial^{\mu} \partial^{\nu} \psi - \frac{\bar{g}}{2} (\bar{\psi} \gamma_{11} \psi)^2 \right], \tag{1}$$

where  $\psi$  denotes a  $d_{\gamma}=32$  component Luttinger spinor and  $\bar{\psi}$  its conjugate  $\bar{\psi}=\psi^{\dagger}h$  with the spin metric h. The action has been constructed in such a way that the corresponding Minkowskian action is real [13]. For given Lorentz indices  $\mu, \nu, G_{\mu\nu}$  denotes a  $d_{\gamma}\times d_{\gamma}$  matrix which is tracefree in Lorentz as well as spin space and satisfies the relativistic version of the Abrikosov algebra [13, 17, 23]

$$\{G_{\mu\nu}, G_{\kappa\lambda}\} = -\frac{2}{d-1}g_{\mu\nu}g_{\kappa\lambda} + \frac{d}{d-1}(g_{\mu\kappa}g_{\nu\lambda} + g_{\mu\lambda}g_{\nu\kappa}),\tag{2}$$

where d denotes the (Euclidean) spacetime dimension. In our formulas, we keep d sometimes general for illustrative purposes, but concentrate on d=4 dimensional spacetime for the concrete application to studies of criticality. The matrices  $G_{\mu\nu}$  can be spanned by a suitable set of Euclidean Dirac matrices  $\gamma_A$ , see Appendix A for further details. For spanning the nine matrices  $G_{\mu\nu}$  together with the spin metric h, in total 10 Euclidean Dirac matrices are required,  $\gamma_1,\ldots,\gamma_{10}$ . The corresponding Dirac algebra thus contains another Dirac matrix  $\gamma_{11}$  which is used to define the interaction channel in (1). Further scalar interaction channels are also possible [22]. In Minkowski space, the model is relativistically invariant by virtue of the algebra (2) together with a mapping of SO(1,3) Lorentz transformations  $\Lambda^{\mu}_{\nu}$  into the spin-base transformations  $\Lambda^{\mu}_{\nu}$  into the SL(32, $\mathbb{C}$ ),  $\Lambda^{\mu}_{\nu} \to S_{\mathrm{Lor}}(\Lambda) \in \mathrm{SL}(32,\mathbb{C})$ . This mapping defines the Lorentz transformations of relativistic Luttinger spinors, see Appendix A of [13] for details.



By means of a Hubbard-Stratonovich transformation, the model of (1) is fully equivalent to a description involving an auxiliary scalar field,

$$S_{\rm FB} = \int d^4x \left[ -\bar{\psi} G_{\mu\nu} \partial^{\mu} \partial^{\nu} \psi - \bar{h} \phi \bar{\psi} \gamma_{11} \psi + \frac{1}{2} \bar{m}^2 \phi^2 \right], \tag{3}$$

which is obvious by using the equations of motion on the classical level or performing the Gaussian functional  $\phi$  integral on a quantum level, provided the matching condition

$$\bar{g} = \frac{\bar{h}^2}{\bar{m}^2} \tag{4}$$

is fulfilled. The action (3) can be the starting point of a mean-field analysis of the fermionic model as performed in [22]. In the present work, we generalize the model by considering a fully dynamical scalar field which we consider as a fundamental quantum degree of freedom. Focusing on the perturbatively renormalizable operators, we investigate the  $\gamma_{11}$  Yukawa model

$$S = \int d^4x \left[ -\bar{\psi}G_{\mu\nu}\partial^{\mu}\partial^{\nu}\psi + \frac{1}{2}\partial_{\mu}\phi\partial^{\mu}\phi - \bar{h}\phi\bar{\psi}\gamma_{11}\psi + \frac{1}{2}\bar{m}^2\phi^2 + \frac{\bar{\lambda}}{8}\phi^4 \right],\tag{5}$$

where we have included a scalar kinetic term and a self-interaction with bare coupling  $\bar{\lambda}$ . Similar to the fermionic model (1), also the  $\gamma_{11}$  Yukawa model features a  $\mathbb{Z}_2$  symmetry: the model is invariant under a simultaneous replacement of  $\psi \to -e^{i\frac{\pi}{2}\gamma_{11}}\psi$ ,  $\bar{\psi} \to \bar{\psi}e^{-i\frac{\pi}{2}\gamma_{11}}$ , and  $\phi \to -\phi$ ; note that  $\psi$  and  $\bar{\psi}$  are independent variables in the quantum theory. This  $\mathbb{Z}_2$  symmetry also inhibits a bare fermionic mass term. Here and in the following, we assume the fermion fields to occur in  $N_f$  flavors.

With both the fermionic field and the scalar field exhibiting a canonical mass dimension of one in d=4, the model features the renormalizable coupling  $\bar{\lambda}$ , the superrenormalizable Yukawa coupling  $\bar{h}$  and the scalar mass parameter  $\bar{m}$  which are a priori independent.

If the  $\mathbb{Z}_2$  symmetry is broken by a scalar expectation value  $\phi \to v$ , the spectra of both fields are gapped: the scalar field exhibits a massive  $\sigma$ -type mode as lowest excitation, whereas the fermions develop an imaginary mass gap at  $\pm i m_\psi^2$  with  $m_\psi^2 = \bar{h}v$  as smallest possible solutions of the dispersion relation  $p^2 = \pm i m_\psi^2$  (ignoring further interactions). The corresponding free fermionic propagator has square root singularities in the complex  $p^2$  plane with a branch cut along the imaginary axis; these, however, combine in closed fermion loops to a gapped  $1/(p^4 + m_\psi^4)$  form yielding well-defined Wick-rotatable momentum integrals, cf. [22].

It is instructive to compare the model (5) with a standard Yukawa model involving, e.g., Dirac fermions. This analogous case features the same three parameters, all of which exert a qualitative and uantitative influence on the low-energy observables [24–28]. For instance, the mass parameter  $\bar{m}^2$  governs the properties of the low-energy phase: for  $\bar{m}^2$  larger than a critical value  $\bar{m}_{\rm cr}^2$ , the model remains in the symmetric phase with a massive scalar and massless fermions and  $\bar{h}$  and  $\bar{\lambda}$  governing their interactions. For  $\bar{m}^2$  smaller than a critical value, the model is in the broken phase with the scalar field acquiring an expectation value v (determined by  $\bar{m}^2$ ), all modes are gapped, and the couplings  $\bar{h}$  and  $\bar{\lambda}$  determine the resulting fermion mass and the mass of the scalar  $\sigma$ -type mode.



Moreover, for generic initial values of the bare mass  $\bar{m}^2$ , say of order of a UV cutoff scale  $\Lambda$ , also the dimensionful low-energy observables, e.g., the vacuum expectation values and the mass spectrum, will be of the order of the cutoff scale. In order to reach a sizable scale separation with  $v \ll \Lambda$ , the bare mass parameter has to be fine-tuned extremely close to the critical value  $\bar{m}_{\rm cr}^2$ . In the language of statistical physics, the standard Yukawa model with Dirac fermions has a second-order (quantum) phase transition with the scalar mass parameter serving as the control parameter. The long-range physics becomes insensitive to the microscopic realization, i.e., the cutoff can be sent to infinity, provided that the model is fine-tuned to criticality. The latter corresponds to non-generic initial conditions, and the fine-tuning has to be done "by hand" for concrete numerical solutions.

By contrast, the model (5) has very different features as we show in the following: the model is critical for generic choices of initial conditions, i.e.,  $v \ll \Lambda$  can be reached without fine-tuning, the system is always in the broken phase, and the low-energy observables are universal to a large degree, i.e., the mass spectrum is independent of the bare parameters for a large region in parameter space. In this region, the model (5) has only one parameter instead of the expected three; this one parameter essentially corresponds to a scale thus reflecting the paradigmatic field theory property of dimensional transmutation.

#### 3 Renormalization Flow

While the model (5) can straightforwardly be analyzed using perturbation theory or effective field theory methods, we use the functional RG in the present work. This method has the advantage of being able to account for threshold phenomena as they can occur in both the symmetric and the broken regime at various scales in the present model. Perturbative or effective-field-theory results are provided by our functional RG analysis in the corresponding simplifying limits.

More specifically, we employ the Wetterich equation [29] describing the RG flow of the effective action  $\Gamma_k$  as a function of an RG scale parameter k,

$$\partial_t \Gamma_k = \frac{1}{2} \text{STr} \left[ \frac{\partial_t R_k}{\Gamma_k^{(2)} + R_k} \right],$$
 (6)

where  $\partial_t = k \frac{d}{dk}$ , and  $R_k$  specifies the Wilsonian momentum-shell regularization, see [30– 35] for details. The bare action (5) of our model serves as the initial condition for  $\Gamma_k$  at a UV scale,  $\Gamma_{k=\Lambda} = S$ . At k=0, the action corresponds to the full quantum effective action, i.e., the 1PI generating functional  $\Gamma_{k=0} = \Gamma$ .

Our approximation to solve the Wetterich equation is based on the ansatz

$$\Gamma_k = \int d^4x \left[ -Z_{\psi}\bar{\psi}G_{\mu\nu}\partial^{\mu}\partial^{\nu}\psi + \frac{Z_{\phi}}{2}\partial_{\mu}\phi\partial^{\mu}\phi - \bar{h}\phi\bar{\psi}\gamma_{11}\psi + U(\phi) \right],\tag{7}$$

where we include a full scale-dependent effective potential U for the scalar field, and also the Yukawa coupling  $ar{h}$  and the wave function renormalizations  $Z_{\psi,\phi}$  are considered to be kdependent. This ansatz corresponds to an improved local potential approximation (so-called



LPA') which can be considered as a leading order in a systematic derivative expansion of the action. This approximation is well tested in a plethora of nonperturbative analyses of Yukawa systems [36–49].

Upon insertion into the Wetterich (6), our ansatz (7) yields flow equations for all k-dependent quantities. It is convenient to express the resulting flows in terms of dimensionless renormalized quantities. For this, we first define the dimensionless effective potential as a function of a dimensionless renormalized field invariant,

$$u(\rho) = \frac{U(\phi)}{k^d}, \quad \rho = \frac{Z_{\phi}}{2} \frac{\phi^2}{k^{d-2}}.$$
 (8)

The dimensionless renormalized Yukawa coupling reads

$$h^2 = \frac{\bar{h}^2}{Z_{\psi}^2 Z_{\phi} k^{6-d}}. (9)$$

The flow of the wave function renormalizations is encoded in the anomalous dimensions

$$\eta_{\psi,\phi} = -\partial_t \ln Z_{\psi,\phi}. \tag{10}$$

Correspondingly, the resulting flows can be written as

$$\partial_t u(\rho) = -d u + (d - 2 + \eta_\phi) \rho u' + 2v_d \left[ l_0^d (u' + 2\rho u''; \eta_\phi) - N_f d_\gamma l_0^{(L) d} (2\rho h^2; \eta_\psi) \right], \quad (11)$$

where primes denote derivatives with respect to the invariant  $\rho$ . The phase space factor  $v_d^{-1}=2^{d+1}\pi^{d/2}\Gamma(d/2)$  reduces to  $v_4=1/(32\pi^2)$  in d=4. Here and in the following, the functions l (and m used below) represent threshold functions which encode the result of the regularized loop integration. For zero arguments, they yield simple positive constants. For large first arguments, they vanish thereby encoding threshold effects. The precise form depends on the choice of the regulator, details are given in Appendix B The flow of the Yukawa coupling yields

$$\partial_t h^2 = -(2 - 2\eta_{\psi} - \eta_{\phi})h^2 + 8v_d h_k^4 l_{1,1}^{\text{(LB)} d} (\omega_1, \omega_2; \eta_{\psi}, \eta_{\phi}), \qquad (12)$$

where

$$\omega_1 = 2 \kappa h^2, \quad \omega_2 = u'(\kappa) + 2\kappa u''(\kappa),$$
(13)

and  $\kappa = \rho_{\min}$  denotes the minimum of the potential such that  $u'(\kappa) = 0$  for  $\kappa \neq 0$ . The anomalous dimensions derived from the flow of the wave function renormalizations are given by

$$\eta_{\psi} = \frac{16}{d(d+2)} v_d h^2 m_{1,2}^{(\text{LB}),d}(\omega_1, \omega_2; \eta_{\psi}, \eta_{\phi}), \tag{14}$$



$$\eta_{\phi} = \frac{8v_d}{d} \kappa (3u'' + 2\kappa u''')^2 m_{2,2}^d(\omega_2; \eta_{\phi}) 
+ \frac{8v_d}{d} N_f d_{\gamma} h^2 \left( m_4^{(L),d}(\omega_1, \eta_{\psi}) - 2h^2 \kappa m_2^{(L),d}(\omega_1, \eta_{\psi}) \right).$$
(15)

Upon insertion of the solutions of (15), (14) into (11), (12), the flow of the scalar potential and of the Yukawa coupling can be integrated and the low energy observables can be determined within the present ansatz.

For a simplified discussion, a polynomial expansion of the potential is useful. In the symmetric regime (SYM), we use an expansion about zero scalar field amplitude, whereas we expand about the nontrivial minimum  $\kappa > 0$  in the symmetry broken regime (SSB),

$$u(\rho) \simeq \begin{cases} \sum_{n=1}^{N_{\rm p}} u_n \rho^n, & (\text{SYM}), \\ \sum_{n=2}^{N_{\rm p}} u_n (\rho - \kappa)^n, & (\text{SSB}), \end{cases}$$
(16)

where  $N_{\rm p}$  specifies the order of the polynomial approximation as well as the number of operators included for the parametrization of the potential. In the simplest approximation,  $N_{\rm p}=2$ , we use

$$u(\rho) \simeq \epsilon \rho + \frac{1}{2} \lambda \rho^2 \text{ (SYM)}, \quad u(\rho) \simeq \frac{1}{2} \lambda (\rho - \kappa)^2 \text{ (SSB)},$$
 (17)

such that  $\epsilon = \frac{\bar{m}^2}{Z_{\phi}k^2}$  denotes the dimensionless renormalized mass,  $\lambda \equiv 2u_2 = \frac{\bar{\lambda}}{Z_{\phi}^2k^{4-d}}$  the renormalized scalar  $\phi^4$  coupling, and  $\kappa = \frac{v^2}{2k^{d-2}}$  is the dimensionless version of the expec-

renormalized scalar  $\phi^*$  coupling, and  $\kappa = \frac{1}{2k^{d-2}}$  is the dimensionless version of the expectation value of the (renormalized) field  $v = \sqrt{Z_{\phi}}\phi_{\min}$  in the SSB regime. Once the RG flows are computed down to low scales k, we can straightforwardly determine estimates for the physical observables. For instance for flows arriving in the phase with spontaneous symmetry breaking, we obtain the vacuum expectation value, the scalar  $\sigma$ -type mass and the fermion mass from

$$v = k\sqrt{2\kappa}|_{k\to 0}, \ m_{\sigma} = k\sqrt{2\lambda\kappa}|_{k\to 0}, \ m_{\psi} = k\sqrt[4]{2\kappa h^2}|_{k\to 0}$$
 (18)

where we have used d = 4, and the fermion mass  $m_{\psi}$  gaps the spectrum of the Luttinger fermions along the imaginary axis in the  $p^2$  plane [22].

## 4 Leading-Order Polynomial Expansion

Several aspects of the RG equations can be studied analytically. Let us first concentrate on the flow of the relevant mass parameter  $\epsilon$  and the marginal couplings  $h^2$  and  $\lambda$ .



In a conventional perturbative expansion, we would focus on the deep Euclidean region by ignoring the threshold effects, i.e., set all arguments of the threshold functions to zero. Using the functional RG flow, it is, however, straightforward to include the threshold phenomena. For definiteness, we perform this first analysis in the symmetric regime, assuming  $\epsilon>0$  and  $\kappa=0$ , implying  $\omega_1=0$ ,  $\omega_2=\epsilon$ . The corresponding expansion of the flow equations of the relevant and marginal couplings yields

$$\partial_t \epsilon = -\left(2 - \eta_\phi\right) \epsilon - \frac{3\left(1 - \frac{\eta_\phi}{6}\right)}{32\pi^2} \frac{\lambda}{(1 + \epsilon)^2} + \frac{N_f d_\gamma \left(1 - \frac{\eta_\psi}{6}\right)}{8\pi^2} h^2,\tag{19}$$

$$\partial_t \lambda = 2\eta_\phi \lambda + \frac{9\left(1 - \frac{\eta_\phi}{6}\right)}{16\pi^2} \frac{\lambda^2}{(1+\epsilon)^3} - \frac{N_f d_\gamma \left(1 - \frac{\eta_\psi}{6}\right)}{2\pi^2} h^4, \tag{20}$$

$$\partial_t h^2 = -\left(2 - 2\eta_\psi - \eta_\phi\right) h^2 + \frac{1}{8\pi^2} \frac{h^4}{(1+\epsilon)} \left[ 2\left(1 - \frac{\eta_\psi}{6}\right) + \frac{1 - \frac{\eta_\phi}{6}}{1+\epsilon} \right]. \tag{21}$$

To this order, the expansion of the anomalous dimensions reads

$$\eta_{\psi} = \frac{\left(1 - \frac{\eta_{\phi}}{2}\right)}{48\pi^2} \frac{h^2}{(1+\epsilon)^2},\tag{22}$$

$$\eta_{\phi} = \frac{5N_{\rm f}d_{\gamma}\left(1 - \frac{\eta_{\psi}}{5}\right)}{16\pi^2}h^2. \tag{23}$$

The one-loop result of all flows in the conventional deep Euclidean region is obtained by setting  $\epsilon = 0$ , i.e., ignoring threshold effects, and upon insertion of  $\eta_{\psi,\phi}$  into (19)-(21) and a subsequent expansion to lowest-coupling order.

## 4.1 Large- $N_{\rm f}$ Analysis

The preceding equations simplify in the limit of a large number of Luttinger flavors  $N_{\rm f}$ . For this, we assume  $N_{\rm f}d_{\gamma}\gg 1$ , but  $N_{\rm f}d_{\gamma}h^2=const$ , implying that  $h^2\sim 1/(N_{\rm f}d_{\gamma})\ll 1$ . Since  $d_{\gamma}=32$ , already  $N_{\rm f}=1$  turns out to satisfy the "large- $N_{\rm f}$ " approximation rather well.

From (22), we deduce that  $\eta_{\psi} \simeq 0$  in this limit, whereas  $\eta_{\phi}$  contributes fully to leading order. Dropping the subleading orders, the Yukawa flow (21) reduces to

$$\partial_t h^2 = -(2 - \eta_\phi)h^2 + \mathcal{O}(1/(N_{\rm f}d_\gamma)),$$
 (24)

independently of the size of  $\epsilon \geq 0$ . For a given value of  $N_{\rm f}$  and upon insertion of  $\eta_{\phi} \sim h^2$ , the right-hand side corresponds to a parabola in  $h^2$  with two zeros. These zeros correspond to fixed points of the RG flow. In addition to the Gaussian, i.e., non-interacting fixed point  $h^2=0$ , we observe the existence of an interacting fixed point at

$$h_*^2 = \frac{32\pi^2}{5N_{\rm f}d_{\gamma}} \Leftrightarrow \eta_{\phi} = 2 \quad \text{for } N_{\rm f}d_{\gamma} \to \infty.$$
 (25)



Inserting this fixed-point value into the flow of the scalar self-interaction (20), also  $\lambda$  exhibits a fixed point at

$$\lambda_* = \frac{128\pi^2}{25N_{\rm f}d_{\gamma}} \quad \text{for } N_{\rm f}d_{\gamma} \to \infty,$$
 (26)

which demonstrates that also  $\lambda_*$  scales like  $\sim 1/(N_{\rm f} d_\gamma)$  in a large- $N_{\rm f}$  analysis. It is straightforward to check that this fixed point is fully IR attractive in the  $(\lambda,h^2)$  plane. This is illustrated in Fig. 1 where phase diagram in terms of a stream plot of the flow towards the IR is depicted in the  $(\lambda,h^2)$  plane.

The corresponding critical exponents, defined in terms of the negative of the eigenvalues of the stability matrix B,

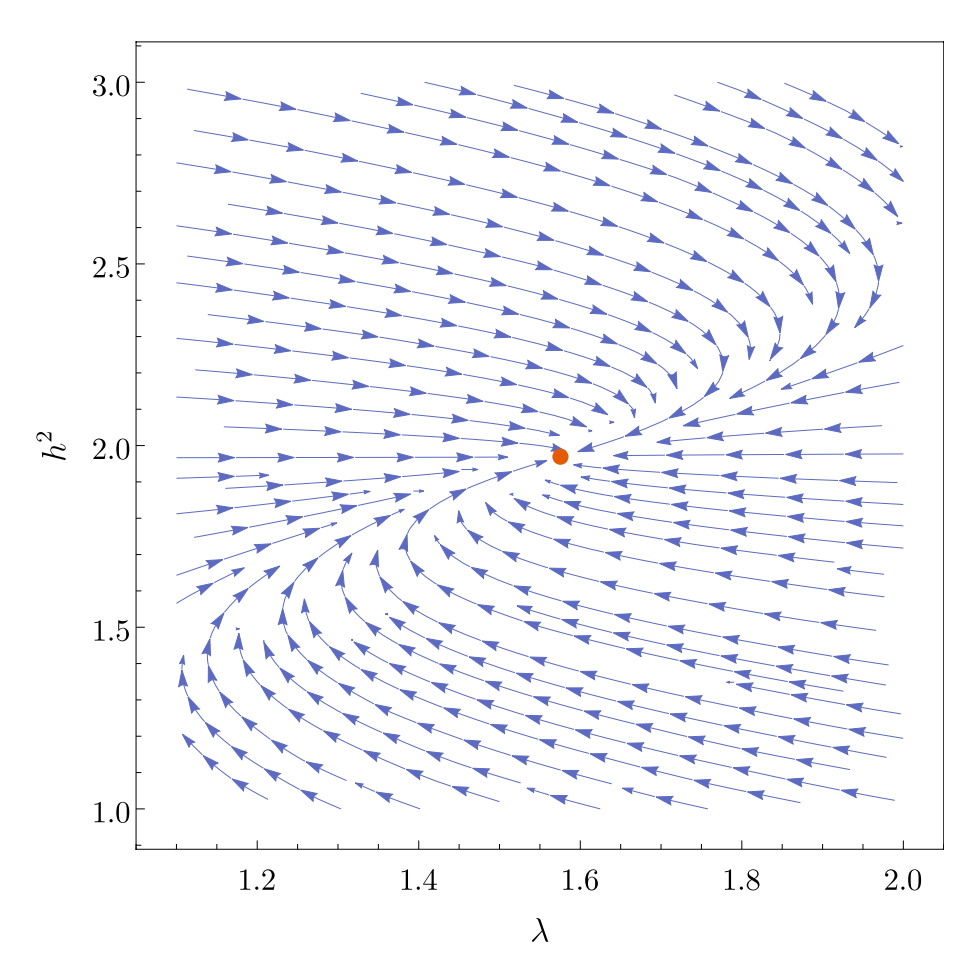


Fig. 1 Phase diagram of the  $\gamma_{11}$  Yukawa model with Luttinger fermions, in the plane of the dimensionless scalar self-interaction  $\lambda$  and the dimensionless Yukawa coupling  $h^2$ . The arrows indicate the RG flow towards the IR. The interacting fixed point, highlighted in red, is fully IR attractive. The flow has been obtained from the full (20)-(21) with  $\epsilon=10$  and for  $N_{\rm f}=1,\,d_{\gamma}=32$ 



$$\theta = -\operatorname{eig}\{B\}, \quad B_{ij} = \frac{\partial(\partial_t g_i)}{\partial g_i}, \quad g_i = h^2, \epsilon, \lambda, \dots,$$
 (27)

are

$$\theta_{h^2} = -2, \quad \theta_{\lambda} = -4, \quad \text{for } N_{\rm f} d_{\gamma} \to \infty,$$
 (28)

which reveals that both couplings are RG irrelevant and their flow is fully governed by the fixed point. Since the exponents are not small, the system approaches the fixed point rather rapidly. In conclusion, the two couplings thus do not represent physical parameters since the long-range behavior is determined by the fixed point.

However, the fixed point is not a quantum scale invariant point of the full system, but only a partial fixed point of the couplings studied so far. Inserting the fixed-point values into the remaining (19), we find to leading order

$$\partial_t \epsilon = \frac{4}{5}, \quad \text{for } N_f d_\gamma \to \infty,$$
 (29)

as a consequence of the large scalar anomalous dimension  $\eta_{\phi}=2$ . The latter, in fact, corresponds precisely to the value that renders the mass parameter from relevant near the Gaussian fixed point to marginal with  $\theta_m=0$  at the partial fixed point. Fixing the initial condition for  $\epsilon$  at the high scale  $\Lambda$  to some value  $\epsilon_{\Lambda}>0$ , the solution to (29) reads

$$\epsilon(k) = \epsilon_{\Lambda} + \frac{4}{5} \ln \frac{k}{\Lambda},\tag{30}$$

which shows that the mass parameter  $\epsilon$  flows logarithmically slowly to smaller values, transitioning into the SSB regime with  $\epsilon(k_{\rm SSB})=0$  at

$$k_{\rm SSB} = \Lambda e^{-\frac{5}{4}\epsilon_{\Lambda}}.\tag{31}$$

We observe that  $k_{\rm SSB} \ll \Lambda$  is natural for generic choices of  $\epsilon_{\Lambda}$ . For instance: in order to have  $k_{\rm SSB}$  being n orders of magnitude smaller than  $\Lambda$ , we only need to choose  $\epsilon_{\Lambda} = n \frac{4}{5} \ln(10) \simeq 1.8 \ n$  as initial condition. No fine-tuning is needed to separate  $k_{\rm SSB}$  from  $\Lambda$ . The initial conditions for  $h^2$  and  $\lambda$  are even less relevant, since they are quickly attracted to the fixed point fairly independently of the initial conditions.

Once  $\epsilon(k)$  has dropped below zero for  $k < k_{\rm SSB}$ , (19)-(22) are no longer valid but have to be replaced by their analogues accounting for a nontrivial minimum  $\kappa$  of the effective potential  $u(\rho)$ . Around  $k \sim k_{\rm SSB}$ , all couplings start to run fast. However, once the (dimensionless) minimum  $\kappa$  grows large, strong threshold effects set in since  $\omega_{1,2} \sim \kappa$ . As a consequence, all threshold functions essentially drop to zero quickly describing the decoupling of massive modes. The flow is then governed only by the dimensional scaling terms and all dimensionful physical observables such as those listed in (18) approach constant values; the flow "freezes out".

We emphasize that the large- $N_{\rm f}$  limit does not feature a symmetric phase, independently of the initial conditions. Of course, large initial values for the scalar mass term  $\epsilon_{\Lambda} \gg 1$ 



282

will lead to a flow in the symmetric regime over a wide range of scales, but the system will unavoidably end in the broken phase as is obvious from (30). In the language of statistical physics, this is reminiscent to the phenomenon of self-organized criticality: independently of how far the seeming control parameter  $\epsilon_{\Lambda}$  is chosen away from a (naively anticipated) critical point, the RG flow drives the system to criticality. The more  $\epsilon_{\Lambda} > 0$  is chosen away from the regime transition  $\epsilon = 0$ , the closer the system approaches the partial fixed point in the  $(h^2, \lambda)$  plane, i.e., the closer is the system tuned to criticality with more pronounced universal features. Nevertheless, the large- $N_{\rm f}$  flow ultimately ends up in the broken phase with all long-range observables being naturally much smaller than the high-energy scale  $\Lambda$ .

The present RG flow shows also some similarity to the scenario of nordic walking proposed in [50] for a 2+1 dimensional solid-state system, and suggested as a novel ingredient for natural high-energy models. The nordic-walking scenario relies on the existence of a flat region in the  $\beta$  function of a relevant coupling. In the proposal of [50], this can be arranged for through the competition between different fluctuation contributions. In the present case, it is the scalar mass term that exhibits nordic-walking behavior by virtue of a fully IR attractive partial fixed point in all couplings; no specific balance between different  $\beta$  function contributions seems necessary.

## 4.2 Perturbative Analysis

The preceding large- $N_{\rm f}$  analysis is, in fact, more general as naively expected, not only because  $N_{\rm f} d_{\gamma}$  is large even for  $N_{\rm f}=1$ . As a justification, let us analyse (19)-(22) perturbatively without specific assumptions about the size of  $N_{\rm f}d_{\gamma}$ . In addition to the polynomial (perturbative) dependence on the couplings  $h^2$  and  $\lambda$ , the equations depend non-linearly on  $\epsilon$ .

In the limit of large  $\epsilon$ , we observe that the right-hand sides of (19)-(22) reproduce exactly the flow equations of the large- $N_{\rm f}$  limit of the preceding subsection. We conclude that the large- $N_{\rm f}$  analysis also applies to the perturbative large- $\epsilon$  regime, the latter potentially receiving  $1/N_{\rm f}$  corrections. Even the fixed-point values  $h_*^2$  and  $\lambda_*$  are perturbatively small for sufficiently large  $N_{\rm f}$ .

In a straightforward naive perturbative expansion for small couplings  $h^2$  and  $\lambda$ , the anomalous dimensions simplify to

$$\eta_{\psi} = \frac{h^2}{48\pi^2(1+\epsilon)^2}, \quad \eta_{\phi} = \frac{5h^2N_{\rm f}d_{\gamma}}{16\pi^2}.$$
(32)

Insertion into the coupling flows (19)-(21) and an expansion to leading order in the couplings would yield the perturbative flows adequately describing the vicinity of the Gaussian fixed point.

Since we are also interested in the non-Gaussian fixed point identified before in the large- $N_{\rm f}$  limit, there is an improved perturbative expansion which is quantitatively more accurate also near the non-Gaussian fixed point. For this, we observe that the non-Gaussian fixed point is characterized by a scalar anomalous dimension  $\eta_{\phi} \simeq 2 + \mathcal{O}(1/N_{\rm f})$ . Also the fixedpoint values for  $h^2$  and  $\lambda$  scale as  $\sim 1/N_{\rm f}$ . Inserting this scaling into (14), we observe that  $\eta_{\psi}$  scales like  $\sim 1/N_{\rm f}^2$  near the non-Gaussian fixed point, but  $\sim h^2$  near the Gaussian one. Therefore, we can describe both fixed points by using the leading-order formulas (32) to lowest perturbative order, but  $\eta_{\psi} \sim 0 + \mathcal{O}(1/N_{\rm f}^2)$  at higher order. Still, we keep  $\eta_{\phi}$  as in



(32) also at higher order, since it appropriately accounts for  $\eta_{\phi} \simeq 2 + \mathcal{O}(1/N_{\rm f})$ . As a result, we obtain

$$\partial_t \epsilon = -\left(2 - \frac{5N_{\rm f}d_{\gamma}}{16\pi^2}h^2\right)\epsilon - \frac{3\lambda}{32\pi^2(1+\epsilon)^2} + \frac{N_{\rm f}d_{\gamma}}{8\pi^2}h^2\left(1 + \frac{5\lambda}{128\pi^2(1+\epsilon)^2}\right),\tag{33}$$

$$\partial_t \lambda = \frac{5N_{\rm f} d_{\gamma}}{8\pi^2} h^2 \lambda - \frac{N_{\rm f} d_{\gamma}}{2\pi^2} h^4 + \frac{9\lambda^2}{16\pi^2 (1+\epsilon)^3} \left( 1 - \frac{5N_{\rm f} d_{\gamma}}{96\pi^2} h^2 \right),\tag{34}$$

$$\partial_t h^2 = -2h^2 + \frac{5N_{\rm f}d_{\gamma}}{16\pi^2}h^4 + \frac{5+3\epsilon}{12\pi^2(1+\epsilon)^2}h^4 - \frac{5N_{\rm f}d_{\gamma}}{768\pi^4(1+\epsilon)^2}h^6. \tag{35}$$

Conventional perturbative results in the deep Euclidean region are obtained keeping only the leading powers in  $h^2$  and  $\lambda$  and by setting  $\epsilon=0$  in the denominator (and in (35) also in the numerator). The few terms that would formally be of higher order, such as the term  $\sim h^2 \lambda$  in (33), the term  $\sim \lambda^2 h^2$  in (34), and the term  $\sim h^6$  in (35) arise from the anomalous dimension  $\eta_{\phi}$ ; they account for the possibility that this anomalous dimension can become large  $\eta_{\phi} \sim \mathcal{O}(1)$  at a non-Gaussian fixed point. Nevertheless, dropping these terms in a pure perturbative spirit would not modify the following results qualitatively.

From (35), it is again obvious that the Yukawa coupling flow has a non-Gaussian fixed point for any  $N_{\rm f}$  and  $\epsilon \geq 0$ ; for instance, ignoring the subleading term  $\sim h^6$  in (35), the fixed-point value assumes the compact form

$$h_*^2 = \left(\frac{5N_{\rm f}d_{\gamma}}{32\pi^2} + \frac{5+3\epsilon}{24\pi^2(1+\epsilon)^2}\right)^{-1}.$$
 (36)

At large- $N_{\rm f}$ , or alternatively large  $\epsilon$ , we rediscover the result of the preceding subsection, (25). However, even in the extreme opposite limit of  $\epsilon=0$  and for  $N_{\rm f}=1$ , the numerical value for  $h_*^2$  deviates from the large- $N_{\rm f}$  limit only by a few percent.

The same conclusion holds for the scalar self-interaction  $\lambda$  also exhibiting a fixed-point  $\lambda_*$  upon insertion of (36) into (34). The somewhat extensive result can be worked out analytically in a straightforward fashion; here we simply note that the large- $N_{\rm f}$  result of (26) is rediscovered in the corresponding limit (and also for large  $\epsilon$ ); in the extreme opposite limit of  $N_{\rm f}=1$  and  $\epsilon=0$ , the result deviates only on the few percent level.

Most importantly, this fixed point in the  $(h^2, \lambda)$  plane remains fully IR attractive for any value of  $N_f$  and  $\epsilon \geq 0$ . This can be read off from the critical exponents for which we now find

$$\theta_{h^2} = -2, \quad \theta_{\lambda} = [-4, -3.940...], \quad \text{(pert.)},$$

where  $\theta_{\lambda}$  as a function of  $N_{\rm f}$  and  $\epsilon$  varies in the given interval on the few percent level; the upper end of the interval is reached for small but finite  $\epsilon$ .

Also within perturbation theory, the fixed point in these couplings is, of course, only a partial fixed point. Once it is approached rapidly in this coupling plane, the remaining perturbative flow of the dimensionless scalar mass parameter reads again

$$\partial_t \epsilon = c_{\epsilon}, \quad \text{(pert.)},$$
 (38)



282

where  $c_{\epsilon} = c_{\epsilon}(\epsilon, N_{\rm f})$  is a slowly varying positive function of  $\epsilon$  and  $N_{\rm f}$  which remains in the vicinity of its large- $N_{\rm f}$  value  $c_{\epsilon}|_{N_{\rm f}\to\infty}=4/5$ , cf. (29). E.g., for  $\epsilon\to\infty$  but any  $N_{\rm f}$ , we find  $c_{\epsilon} = (4/5) - 1/(20N_{\rm f})$ . In the opposite limit with  $\epsilon = 0$  and  $N_{\rm f} = 1$ ,  $c_{\epsilon}$  is only about 1 percent larger.

In summary, our conclusions of the large-N<sub>f</sub> analysis remain valid in the whole perturbative domain: the Yukawa system develops a partial IR attractive fixed point that is rapidly approached by the Yukawa coupling and the scalar self-interaction for any initial value in the perturbative domain. At this partial fixed point, the scalar mass is no longer a relevant direction, but it is only marginal featuring a logarithmically slow running towards the regime of chiral symmetry breaking. Again, we conclude that a large scale separation  $k_{\rm SSB} \ll \Lambda$  is natural for generic choices of the initial conditions.

## 5 Functional RG Flow

Let us now integrate the functional flows (11)-(15) without any assumption on the size of  $N_{\rm f}$ or the values of the couplings. While there are powerful methods available to solve also the potential flow (11) as a partial differential equation in field space [51-59], we use a simple polynomial expansion about the minimum as parametrized in (16). This gives us access to the spectral information of the Yukawa system, and we can monitor the convergence of this expansion as a function of the polynomial order  $N_{\rm p}$ .

At the initial scale  $k = \Lambda$ , we impose nontrivial initial conditions on all perturbatively marginal or relevant couplings necessary in order to render the theory fully interacting, i.e., choose initial values for  $\epsilon_{\Lambda}$ ,  $h_{\Lambda}^2 > 0$ ; for simplicity, we set all other  $u_{n \geq 2} = 0$  (including  $\lambda_{\Lambda}$ ) at  $k=\Lambda$ , as these couplings are generated by the flow anyway. However, since all scalar couplings are quickly attracted by their corresponding partial fixed point with a large negative (RG irrelevant) critical exponent, generic nontrivial initial conditions for all other  $u_{n>2}$  do not take any relevant influence on the results.

As for the initial conditions for  $\epsilon_{\Lambda}$  and  $h_{\Lambda}^2$ , there are qualitatively two resulting flows: for negative  $\epsilon_{\Lambda} < 0$  (or small  $\epsilon_{\Lambda} > 0$  with sufficiently large  $h_{\Lambda}^2$ ), the flow starts in (or runs comparatively quickly into) the broken regime where all modes become massive and decouple quickly. In this case,  $k_{
m SSB} \lesssim \Lambda$  remains fairly close to the high scale. The resulting dimensionful quantities such as the vacuum expectation value v or the particle masses  $m_{\sigma}$  or  $m_{\psi}$  depend strongly on the details of the initial conditions. In this case, the RG flow is not governed by a (partial) fixed point, hence we do not observe nor expect universal features.

By contrast, for sufficiently large mass parameter, say  $\epsilon_{\Lambda} \gtrsim O(1)$ , and perturbative or medium large initial Yukawa couplings  $h^2_{\Lambda}$ , the RG flow of all other couplings is attracted by the partial fixed point present in all couplings  $h, \lambda = u_2$ , and all other  $u_n$ , while  $\epsilon$  runs logarithmically slowly towards zero and then into the SSB regime, such that  $k_{\rm SSB} \ll \Lambda$ . No fine-tuning of any of the parameters is needed for this generic situation; in fact, the deeper we put the system into the symmetric regime, e.g., with a large positive  $\epsilon_{\Lambda}$ , the more RG time the systems spends near the partial fixed point and is ultimately driven to criticality. As the partial fixed point renders all other couplings RG irrelevant, the IR observables show a large amount of universality, and we can express all dimensionful quantities in units of a single scale.

The degree of universality of the long-range observables is governed by the RG time spent at the partial fixed point; for a simple estimate, we use the RG time scale  $t_{\rm SSB} = \ln \frac{k_{\rm SSB}}{\Lambda}$ 



where the system runs into the broken regime as a proxy for the time spent near the fixed point. Since the irrelevant perturbations near the fixed point die out with their corresponding critical exponents, the non-universal corrections contribute at most with the largest exponent  $\theta_{h^2}=-2$ , cf. (28), such that corrections to universality scale maximally with  $\sim (k_{\rm SSB}/\Lambda)^2$ . Therefore,  $2(\log_{10}e)|t_{\rm SSB}|\simeq 0.82|t_{\rm SSB}|$  serves as an estimate for the number of digits of a long-range observable that are unaffected by non-universal corrections. In Fig. 2, we depict the curves in the  $(h_{\Lambda}^2,\epsilon_{\Lambda})$  plane of initial conditions for which we obtain  $t_{\rm SSB}=-5,-10,-20$  for the  $N_{\rm f}=1$  ( $d_{\gamma}=32$ ) model. The shaded regions above these curves exhibit universality of the long-range observables at least to this estimated degree. Also, we haven't found any significant influence of the initial condition for the scalar interaction  $\lambda_{\Lambda}$  on these curves. This is in agreement with the even more subleading critical exponent  $\theta_{\lambda}\simeq -4$  which induces a rapid die out of the scalar self-coupling. In conclusion, a large region in the space of initial parameters leads to universal long-range physics. This justifies to call these initial conditions generic. No fine-tuning is needed at all to put the system into this region.

As we are mainly interested in this universal regime which we interpret as the analogue of self-organized criticality of dynamical systems, we initialize the flow such that the system spends sufficient RG time  $t=\ln\frac{k}{\Lambda}$  in the symmetric regime, in order for the couplings to be sufficiently attracted by the fixed point, before entering the broken regime. The preceding considerations have also been confirmed by fully numerical tests demonstrating that  $t_{\rm SSB} \lesssim -10$ , i.e.  $k_{\rm SSB}/\Lambda \lesssim 10^{-5}$ , is sufficient to suppress non-universal corrections within our numerical accuracy. For concrete computations, we set  $h_{\Lambda}^2=1$ ,  $u_{n,\Lambda}=0$  and choose  $\epsilon_{\Lambda}$  such that the universal regime will always be reached. For the cases  $N_{\rm f}=1,2$ ,  $\epsilon_{\Lambda}$  has been set to 10. For larger  $N_{\rm f}$ , the initial condition  $\epsilon_{\Lambda}$  has been chosen somewhat larger such that the transition time  $t_{\rm SSB} \lesssim -10$ . This is, because larger  $N_{\rm f}$  for  $h_{\Lambda}^2$  fixed correspond to large initial values for  $\eta_{\phi}$ , cf. for instance (32), inducing a faster initial running until the couplings have sufficiently approached their fixed point values.

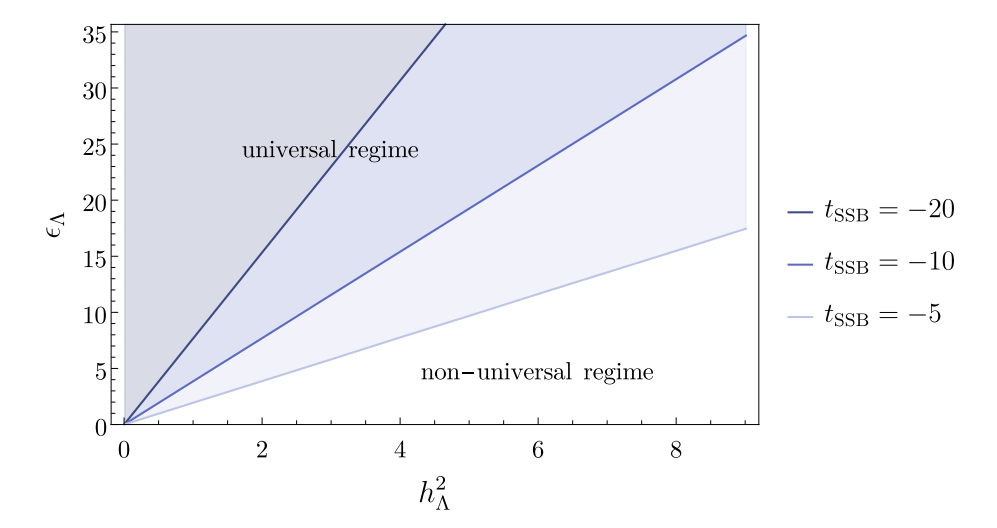


Fig. 2 Degree of universality in the  $(h_{\Lambda}^2, \epsilon_{\Lambda})$  plane of initial conditions for the  $N_{\rm f}=1(d_{\gamma}=32)$  model. The solid curves mark initial conditions for which  $t_{\rm SSB}=-5,-10,-20$ . The shaded regions above these curves correspond to generic initial conditions with a correspondingly increasing degree of universality. (The initial values of all the irrelevant couplings  $u_{n\geq 2}$  are set to zero, but do not exert a significant influence on the data anyway, see text). In subsequent studies, we use  $t_{\rm SSB} \leq -10$  exhibiting a degree of universality sufficient for all practical purposes



In Fig. 3, we plot the resulting dimensionful effective potential as a function of the dimensionful field invariant both in units of the vacuum expectation value  $\nu$  for various values of  $N_{\rm f}$ . In all cases, the potential develops a nontrivial expectation value. Using d'Alembert's ratio test, we have performed an estimate for the convergence radius of the polynomial expansion. Going up to  $18^{\rm th}$  order in the expansion, the ratio test suggests that the convergence radius is of the order 0.005 (in units of  $\nu$ ); the corresponding highest-order results are shown in Fig. 3. (NB: The polynomial expansion is not able to resolve the convexity property of the effective potential. The full flow of (11) would lead to a convex potential, implying that the potential to the left of the minimum in Fig. 3 would become flat in the limit  $k \to 0$  [58, 60–63].)

On the basis of this numerical control of the full flow of the effective potential near its minimum, we can straightforwardly determine the mass of the  $\sigma$ -like scalar excitation  $m_\sigma$  as well as the fermionic mass gap  $m_\psi$  according to (18). In the universal regime, their scale is clearly set by the vacuum expectation value v as well. Since the RG flow of the coupings  $\lambda$  and  $h^2$  is governed by the partial fixed point for a wide range of scales, the partial fixed point for these couplings also exerts an influence on the final mass values. Once, the scalar mass parameter  $\epsilon$  crosses zero at  $k_{\rm SSB}$ , the couplings depart from their fixed-point values such that the details of the SSB flow ultimately determine the mass spectrum quantitatively. For  $N_{\rm f}=1$ , the resulting values for the mass spectrum are shown in Fig. 4 as a function of the approximation order  $N_{\rm p}$  in units of the vacuum expectation value v. While small values of  $N_{\rm p}$  exhibit somewhat larger truncation artefacts, the convergence with increasing order of the truncation appears satisfactory; in particular for the highest orders  $N_{\rm p}=20,22$ , the variation is on the sub-permille level. Quantitatively, we find  $m_\sigma/v \simeq 1.36$  for the sigmalike mass of the scalar excitation and  $m_\psi/v \simeq 1.72$  for the fermionic mass gap.

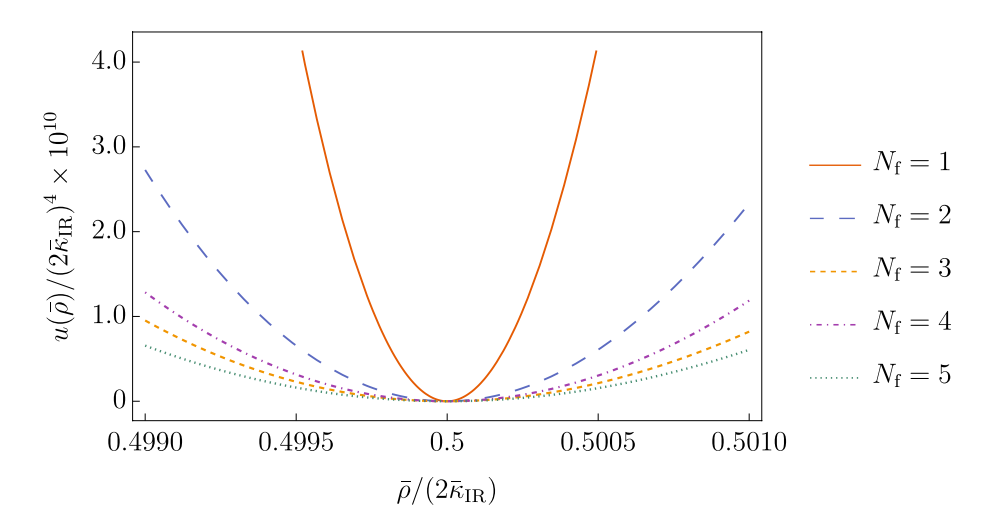


Fig. 3 Dimensionful effective potential of our Yukawa model with Luttinger fermions as a function of the field amplitude  $\rho=\frac{1}{2}\phi^2$  for different values of  $N_{\rm f}$  and  $d_{\gamma}=32$  in units of the resulting vacuum expectation value v. A polynomial expansion at  $18^{\rm th}$  order of the potential has been used, and initial conditions at the UV scale  $\Lambda$  have been chosen such that the flow spends a sufficently wide range of scales near the partial fixed point; no fine-tuning is needed for this while the resulting potential is universal, i.e., essentially independent of the microscopic initial conditions. The figure displays the limited range of field values where the polynomial expansion passes D'Alembert's ratio test for convergence



The dashed lines indicate the would-be value of the masses if computed from the partial fixed point values  $h_*^2$ ,  $\lambda_*$  of (25), (26) in the large- $N_{\rm f}$  limit. More precisely, the estimate for  $m_{\sigma}/v$  indicated by the blue dashed line corresponds to  $m_{\sigma}/v \simeq \sqrt{\lambda_*} = \frac{2\pi}{5}$ , using (18) and the large- $N_{\rm f}$  limit fixed-point value (26); a similar estimate for  $m_{\psi}/v$  involves to choose a scale, since the Yukawa coupling in the original action is dimensionful. The relevant scale here is  $k_{\rm SSB}$ , since this is the scale where the system starts departing from the partial fixed point and subsequently decouples. Hence, the red dashed line in Fig. 4 is given by the estimate  $m_{\psi}/v \simeq \frac{\sqrt[4]{h_*^2 k_{\rm SSB}^2}}{\sqrt{v}}$ , where we use the large- $N_{\rm f}$  limit fixed-point value (25) in addition to the numerical data for  $k_{\rm SSB}$  and  $\nu$ . Since the deviations from finite- $N_{\rm f}$  corrections are on the few percent level, cf. (36), the visible difference of the full numerical result (dots) from the estimates (dashed lines) in Fig. 4 is a result of the full RG flow in the threshold regime  $\epsilon \lesssim 0$ . The fact that this difference is only on the O(10%) level justifies the interpretation that the properties of the long-range observables are essentially governed by the properties of the partial fixed point. Even though the fixed point is destroyed in the course of the transition to the SSB regime, the hierarchy of the couplings is essentially preserved in the course of the flow through the threshold regime.

The mass ratio  $m_\sigma/m_\psi$  is a particularly relevant prediction of our model for several reasons: from the viewpoint of the high-energy completion of the model discussed Section 6 below, the scalar could arise as bi-fermionic bound state. In this context, the deviation of the ratio from  $m_\sigma \simeq 2m_\psi$  is a measure for the binding energy of the scalar state. Also, for a comparison with other nonperturbative methods, we expect the mass ratio

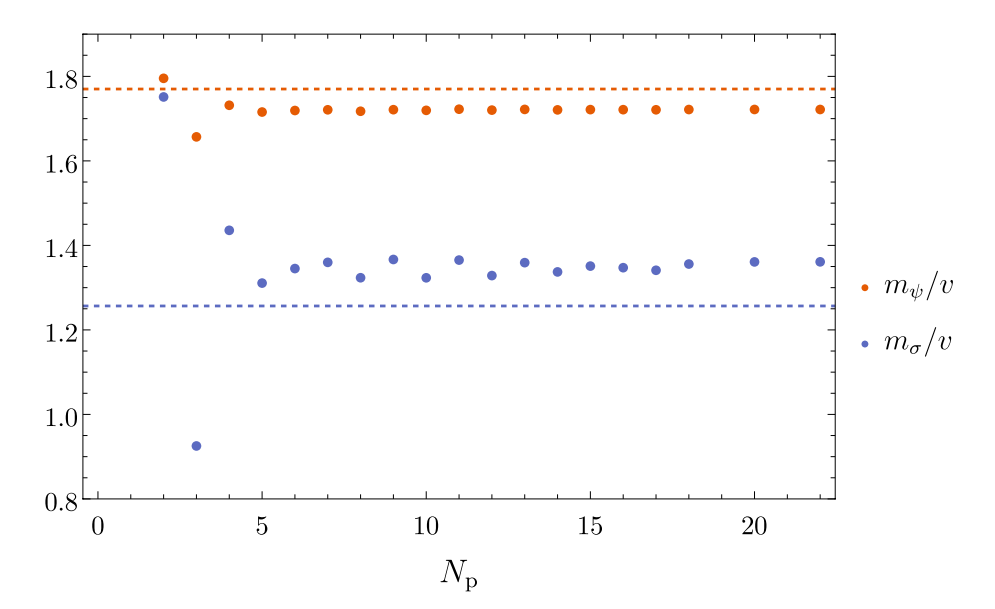


Fig. 4 Ratio of the scalar  $\sigma$ -type mass  $m_{\sigma}$  and the vacuum expectation value  $\nu$  (orange) and ratio of the fermionic mass gap  $m_{\psi}$  and  $\nu$  (blue) for the  $N_{\rm f}=1$  model ( $d_{\gamma}=32$ ) as a function of the polynomial expansion  $N_{\rm p}$ . The initial conditions have been chosen such that the model is in the universal regime. The dashed lines (in the corresponding colors) correspond to an estimate based on the fixed point analysis in the large  $N_{\rm f}$  limit, c.f. (25) and (26), as explained in the main text



282

to play a useful role; e.g., lattice simulations typically have a direct access to spectral information via the study of spatial correlation functions. Our result for the mass ratio is shown in Fig. 5 as a function of the flavor number  $N_{\rm f}$  and for the highest truncation order  $N_{\rm p}=22$ . As expected, we observe a variation on the percent level for small  $N_{\rm f}$ , rapidly converging for larger  $N_{
m f}$ . The mass ratio shown in the plot for  $N_{
m f}=5$  agrees already on the per-mille level with  $m_{\sigma}/m_{\psi} \simeq 0.786$  computed for  $N_{\rm f}=100$  as a large- $N_{\rm f}$  reference

From the viewpoint of the high-energy completion of the model where the scalar is a bifermionic bound state, we conclude that the mass ratio near  $m_{\sigma}/m_{\psi} \simeq 0.79 < 2$  points to a deeply bound relativistic state where the binding energy exceeds the mass gap of a single fermionic constituent.

Finally, the property of self-organized criticality can also be read off from the flow of the scalar anomalous dimension. A typical flow is depicted in Fig. 6 for initial conditions in the universal regime ( $\epsilon_{\Lambda} = 10, h_{\Lambda}^2 = 1, u_{n \geq 2} = 0$ ) and the case  $N_f = 1$ . Near the cutoff  $k \lesssim \Lambda$   $(t \lesssim 0)$ , the flow rapidly approaches the fixed-point value  $\eta_{\phi} \simeq 2$  and remains there for a wide range of scales. This goes hand in hand with the fact that the scalar mass parameter no longer is a relevant operator but becomes marginal at the partial fixed point where it runs logarithmically slowly towards the broken regime quantitatively similar to the large- $N_{\rm f}$  flow (29). At the same time,  $\eta_{\phi} \simeq 2$  induces the partial fixed points in all other couplings  $h^2, \lambda, u_{n>2}$  while keeping  $\eta_{\psi}$  numerically small as expected from (22). This fixed-point controlled flow stops, once  $\epsilon$  drops below

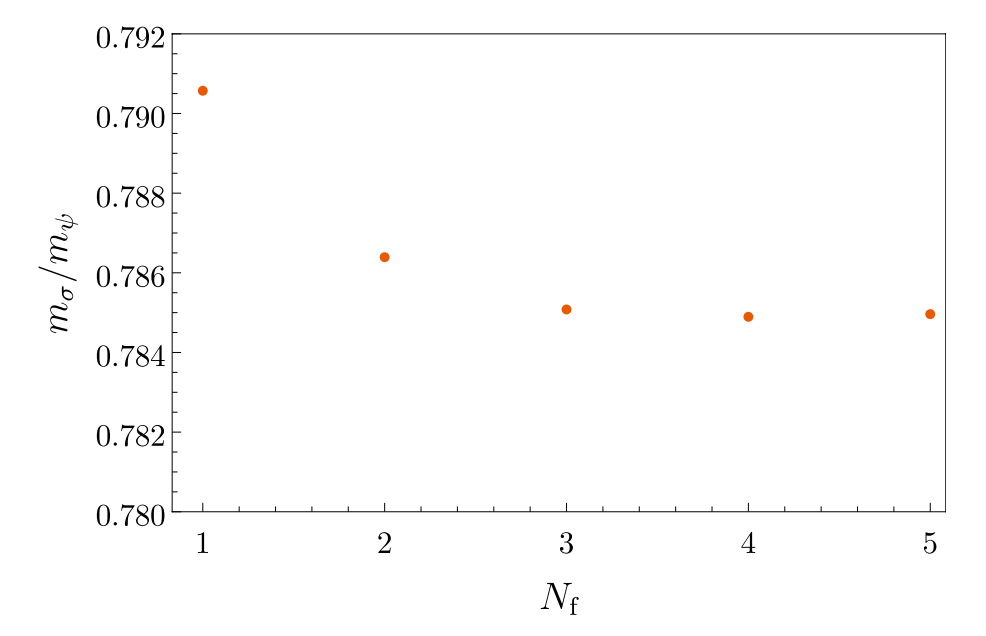


**Fig. 5** Ratio between the scalar  $\sigma$ -type mass  $m_{\sigma}$  and the fermion mass  $m_{\psi}$  as a function of the flavor number  $N_{\rm f}$  ( $d_{\gamma}=32$ ). All data points have been produced within the  $N_{\rm p}=22$  truncation inside the universal regime



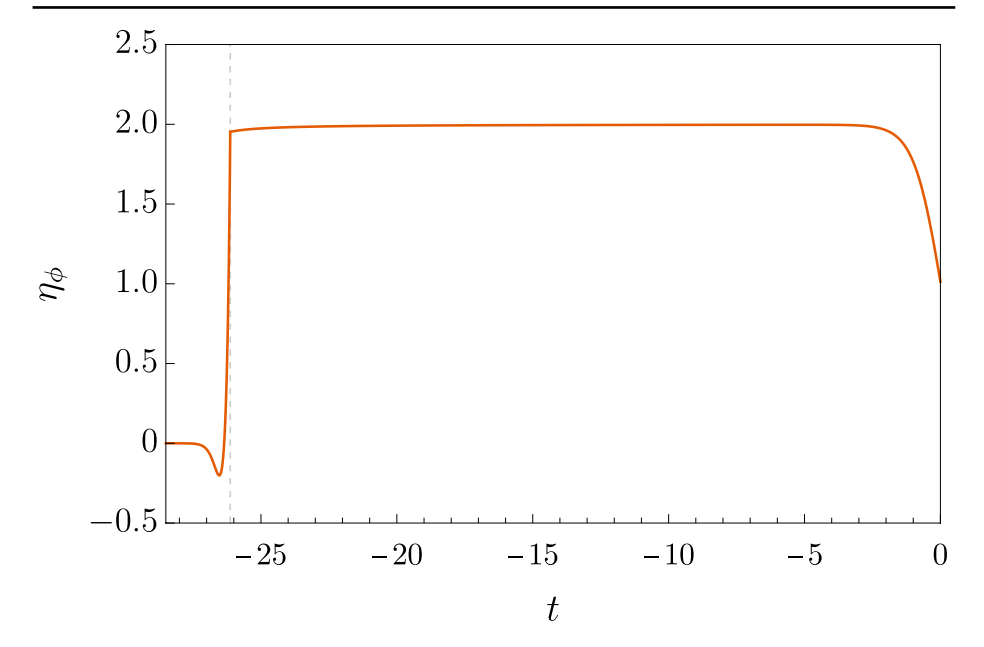


**Fig. 6** Scalar anomalous dimension  $\eta_{\phi}$  for a typical RG flow initiated in the universal parameter space. The plot should be read from right to left (UV to IR): starting in the symmetric regime at t = 0 ( $k = \Lambda$ ),  $\eta_{\phi}$  rapidly approaches the fixed-point value  $\eta_{\phi}=2$ , c.f. (25), and remains there for a wide range of scales. After entering the broken phase towards small t,  $\eta_{\phi}$  vanishes due to threshold effects. This plot uses  $N_{\rm f}=1, d_{\gamma}=32, N_{\rm p}=18, \epsilon_{\Lambda}=10, h_{\Lambda}^2=1, u_{n\geq 2}=0$ , yielding a transition scale of  $t_{\rm SSB}\approx -26$ , i.e.,  $k_{\rm SSB}\simeq 5\times 10^{-12}\Lambda$ , as indicated by the gray dashed line

zero, which in the case of Fig. 6 happens at exponentially small scales near  $t_{\rm SSB} \approx -26$ , i.e.,  $k_{\rm SSB} \simeq 5 \times 10^{-12} \Lambda$ . Here,  $\eta_{\phi}$  starts to run fast towards zero. Once the RG scale drops below the scale of the vacuum expectation value, all modes become massive and decouple which implies that  $\eta_{\phi} \to 0$  for  $t < t_{\rm SSB}$ .

Comparing the results for our model with the scenario for self-organized criticality in chiral Higgs-Yukawa models suggested by Bornholdt and Wetterich in [12], the scalar anomalous dimension  $\eta_{\phi}$  plays the role of the mass anomalous dimension  $\omega$  defined in [12]. The quantitative criterion for self-organized criticality suggested in [12] (Bornholdt-Wetterich criterion),

$$\langle \omega \rangle = \frac{1}{t_0} \int_0^{t_0} dt \ \omega(t) \simeq 2, \quad t_0 := \ln \frac{v}{\Lambda},$$
 (39)

is evidently satisfied for  $\omega = \eta_{\phi}$ , as the scalar anomalous dimension is essentially constant in t and governed by the partial fixed point value  $\eta_{\phi} \simeq 2$ . While (39) could be satisfied also by a varying function  $\omega(t)$ , our Yukawa model based on Luttinger fermions satisfies the Bornholdt-Wetterich criterion in a straightforward fashion. In contrast to the scenario developed in [12], our model bridges the wide ranges of scales between  $k = \Lambda$  and  $k \simeq v$  fully in the symmetric regime. A flow in the broken regime with  $\kappa > 0$  or an attractive partial fixed point with  $\kappa \to \kappa_*$  as studied in [12] is not needed for self-organized criticality as featured by our model.



## 6 High-Energy Completion of the Model

So far, we have studied the flow towards the IR, assuming that the microscopic parameters of the model have been fixed at some initial high-energy scale  $\Lambda$ . The Yukawa model exhibits a remarkable degree of universality as its long-range physics is governed by a partial IR fixed point which is fully IR attractive apart from the marginal mass-parameter direction.

Let us now concentrate on the high-energy behavior of the model by addressing the question as to whether RG trajectories exist along which we can take the limit  $\Lambda \to \infty$ . If so, the corresponding model is UV complete and could exist on all length scales.

From the properties of the IR fixed point, we can already conclude that its UV flow is fully repulsive in the Yukawa and all scalar self-couplings. Therefore, the only RG trajectories for which we may have full UV control are those that emanate from the partial fixed point. Other options would require the existence of further UV fixed points; however, we haven't found any other fixed point in the validity regime of our approximation except for the Gaussian one which would yield a trivial free theory. The fact that all Yukawa and scalar self-couplings are irrelevant at the partial fixed point implies that they are also irrelevant for UV-complete flows emanating from the fixed point. The only physical parameter to be fixed is the mass parameter. We know from the preceding studies that the mass direction runs logarithmically if the other couplings are at the partial fixed point. Towards the UV, the mass parameter  $\epsilon$  runs logarithmically to  $+\infty$  for  $k\to\infty$ .

It is useful to study the flow of the ratio

$$g = \frac{h^2}{\epsilon},\tag{40}$$

which corresponds to the renormalized version of the matching condition of the partially bosonized purely fermionic  $\gamma_{11}$  model (with nondynamical scalars and zero scalar self coupling) [22]. We can straightforwardly derive the flow of this ratio in the present Yukawa model from (19) and (21), yielding

$$\partial_t g = 2\eta_{\psi} g + \frac{3}{32\pi^2} \left( 1 - \frac{\eta_{\phi}}{6} \right) \frac{\lambda}{\epsilon (1+\epsilon)^2} g$$

$$- \frac{1}{8\pi^2} \left[ N_{\rm f} d_{\gamma} \left( 1 - \frac{\eta_{\psi}}{6} \right) - \frac{\epsilon}{1+\epsilon} \left( \left( 2 - \frac{\eta_{\psi}}{3} \right) + \frac{1 - \frac{\eta_{\phi}}{6}}{1+\epsilon} \right) \right] g^2. \tag{41}$$

In order to understand the high-energy behavior, we note that  $\epsilon$  grows large, implying  $\eta_{\psi} \to 0$ , while the coupling  $\lambda$  approaches the fixed point and thus remains bounded, as does  $\eta_{\phi}$ . In the limit  $\epsilon \to \infty$ , we obtain

$$\partial_t g = -\frac{1}{8\pi^2} (N_{\rm f} d_{\gamma} - 2)g^2 \tag{42}$$

which corresponds precisely to the flow of the fermionic self-coupling in the  $\gamma_{11}$  model including the anticipated  $1/N_{\rm f}$  corrections [13, 22].



Therefore, we can interpret the UV complete RG trajectories present in our Yukawa model as follows: the flow of the Yukawa coupling dominated by the partial fixed point and the logarithmic running of the scalar mass parameter are reflections of the asymptotic freedom of the purely fermionic  $\gamma_{11}$  model. The latter is UV complete, features dimensional transmutation, and exhibits the same long-range behavior as our Yukwawa model. We conclude that the UV complete trajectories in our Yukawa model and the fermionic  $\gamma_{11}$  model are in the same universality class, since they are governed by the same fixed point. As our preceding discussion has demonstrated, the models are also in the same universality class even if the Yukawa model is initiated with generic initial conditions. This is because the partial fixed point is fully IR attractive in those couplings that would induce deviations from the purely fermionic description. Of course, if the Yukawa model serves as an effective field theory fixed at an initial UV scale  $\Lambda$ , the long-range physics can deviate from the universal trajectory by corrections of the order  $\sim 1/\Lambda^{|\theta_i|}$ , where  $\theta_i$  corresponds to a suitable exponent of the irrelevant operators.

The effective-field theory viewpoint also illustrates that the existence of a UV completion is a priori unrelated to the property of self-organized criticality: for this let us assume that a corresponding Yukawa theory with Dirac fermions was UV complete, e.g., with the Yukawa couling and the  $\phi^4$  compling rendered asymptotically free by some mechanism. The corresponding couplings would still be marginal parameters of the theory, and, most importantly, the scalar mass would still be a relevant parameter requiring a fine-tuning of initial conditions in order to separate an initial UV scale  $\Lambda$  from a gapped low-energy regime. By contrast, our present Yukawa model renders the scalar mass parameter marginal (and all other couplings irrelevant) by virtue of the quasi fixed point, thereby manifesting properties of self-organized criticality.

This interpretation is also corroborated by the scalar anomalous dimension being  $\eta_{\phi} \simeq 2$ near the partial fixed point. This implies that the scalar wave function renormalization behaves like

$$Z_{\phi}(k) \simeq Z_{\phi}(k_{\mathrm{IR}}) \frac{k_{\mathrm{IR}}^2}{k^2}, \quad \text{for } k \to \infty$$
 (43)

for  $k_{\rm IR}$  representing some IR scale at which the field amplitude is renormalized. For instance, normalizing the wave function renormalization naturally to  $Z_{\phi}(k_{\rm IR})=1$  in the long-range limit, the wave function renormalization becomes small towards the UV. The kinetic term of the scalars thus becomes suppressed and the scalar field more and more resembles a nondynamical auxiliary field, similarly to that introduced by a Hubbard-Stratonovich transformation of a fermionic self-interaction. Of course, near the transition scale  $k \simeq k_{\rm SSB}$ ,  $\eta_{\phi}$ deviates from  $\eta_{\phi} \simeq 2$  and approaches  $\eta_{\phi} \simeq 0$  for  $k \ll k_{\rm SSB}$ , implying that (43) receives some quantitative corrections; however, the scaling with  $\sim 1/k^2$  towards higher energies holds true over the range of scales where the system is close to the partial fixed point.

Finally, the present fermionic picture also offers an explanation for the fact that the curves of constant  $t_{\rm SSB}$  in Fig. 2 have almost constant slope: in the fermionic language,  $t_{\rm SSB}$  essentially corresponds to the scale of the IR divergence of the coupling g when integrating the flow (42) towards the IR. Now, changing the initial conditions for  $\epsilon_{\Lambda}$  and  $h_{\Lambda}^2$  such that their ratio  $g_{\Lambda} = h_{\Lambda}^2/\epsilon_{\Lambda}$  remains fixed, leaves the scale for the IR divergence of g unchanged. The universal region in the full Yukawa model – if reduced to the UV-complete trajectory – thus corresponds to initial conditions of the fermionic model in the perturbative weak coupling regime.



282

## 7 Conclusions

The relativistic Yukawa model proposed in this work exhibits features that are both novel and, to the best of our knowledge, unprecedented in quantum field theories in four-dimensional spacetime. In contrast to conventional models involving Dirac, Majorana or Weyl fermions, the use of relativistic Luttinger fermions exerts a strong influence on the RG phase diagram of the model in the space spanned by the power-counting RG relevant and marginal couplings: for generic initial conditions (including those with an arbitrarily positive scalar mass parameter in units of the cutoff scale), the model features an IR attractive partial fixed point of the RG evolution at which the system can bridge a wide range of scales. While all couplings are RG irrelevant at the fixed point, the scalar mass parameter is RG marginal and exhibits a slow logarithmic drift towards small values.

The long-range behavior of the model is characterized by spontaneous symmetry breaking and mass gap generation in both the scalar and the fermionic sector. Remarkably, the low-energy scales such as the scalar condensate or mass gaps can be many orders of magnitude smaller than a microscopic UV cutoff scale without the need to fine-tune initial parameters. In fact, the UV and IR scales are naturally many orders of magnitude apart for generic initial conditions, including those with couplings of order one and a scalar mass parameter of the order of several times the UV cutoff scale.

Some of these exceptional properties of our Yukawa model are reminiscent to the phenomenon of self-organized criticality in statistical or dynamical systems: identifying the RG time with the physical time in dynamical systems, our model inevitably runs towards a scale where it becomes critical in the sense of an onset of spontaneous symmetry breaking. At this scale, all modes are gapless featuring large fluctuations. For generic initial conditions, the long-range behavior is universal because of the IR attractiveness of the partial fixed point at which the dependence of the system on its initial condition is depleted and largely removed. The partial fixed point is characterized by critical exponents governing the RG running of the dimensionless couplings in terms of simple power-laws. The most prominent similarity to self-organized criticality is given by the slow logarithmic running of the (dimensionless) scalar mass parameter which plays the role of a slow driving force that gradually and inevitably moves the model to criticality.

The present model therefore is a concrete realization of a scenario envisaged in [12] for addressing the issue of naturalness in elementary particle physics in terms of self-organized criticality. Whether or not the present mechanism can be used for corresponding model building in elementary particle physics is an open question. Possible pathways include adding a separate Luttinger fermionic sector to the standard model, or embedding its fermionic content into Luttinger spinors; for a first assessment see [13]. While speculative, it might be an inspiring observation to see that the universal scalar-to-fermion mass gap ratio of our model is quantitatively close to the Higgs-to-top mass ratio in the standard model.

Within the functional RG approach, we have been able to derive this mass-gap ratio together with a number of quantitative results for the mass spectrum. Provided the model spends sufficient RG time near the partial fixed point, as is the case for generic initial conditions, the long-range properties of the model are universal. While some of our nonperturbative results can also be verified with large- $N_{\rm f}$  techniques as used in this work as well, we believe that these quantitative long-range properties could be a prime example for the application of other techniques such Dyson-Schwinger or gap equations, or lattice field theory.



Such techniques can also shed further light on the nature of the fermionic mass gap in our model which occurs in the form of square root singularities with a branch cut along the imaginary axis in the (Minkowskian) complex  $p^2$  plane and the question of the existence or inexistence of Luttinger fermions as asymptotic states [22]. Since such propagators do not feature a Lehmann-Källen spectral representation, we cannot draw an immediate conclusion about the positivity of the Hilbert space. Therefore, it is also an open question as to whether relativistic Luttinger fermions satisfy the spin-statistics or the CPT theorem. These questions may best be addressed in a Hamiltonian approach to quantization.

Finally, an attractive feature of our model is that it features a UV complete extension by virtue of the asymptotically free purely fermionic model which is in the same universality class as our Yukawa model. Though our results for the Yukawa model are independent of this possible UV completion, the existence of such a scale-invariant high-energy limit may represent another motivation to explore such models with relativistic Luttinger fermions even further.

## Appendix A: Abrikosov Algebra

For completeness, we recall a few aspects of the Abrikosov algebra [23] in (2) in a relativistic context as studied in [13, 22].

While not explicitly needed, it is helpful to know that a representation of the  $G_{\mu\nu}$  matrices can be constructed in terms of a Euclidean Dirac algebra  $\{\gamma_A,\gamma_B\}=2\delta_{AB}$ . For the present work, we work in four-dimensional Euclidean spacetime with metric  $g=\mathrm{diag}(1,1,1,1)$ , such that the Abrikosov algebra is satisfied by

$$G_{0i} = -\sqrt{\frac{2}{3}}\gamma_{A=i}, \quad i = 1, 2, 3,$$

$$G_{12} = -\sqrt{\frac{2}{3}}\gamma_{4}, \quad G_{23} = -\sqrt{\frac{2}{3}}\gamma_{5}, \quad G_{31} = -\sqrt{\frac{2}{3}}\gamma_{6},$$

$$G_{00} = -\gamma_{7}, \quad G_{11} = -\frac{1}{3}\gamma_{7} - \frac{2\sqrt{2}}{3}\gamma_{8},$$

$$G_{22} = -\frac{1}{3}\gamma_{7} + \frac{\sqrt{2}}{3}\gamma_{8} - \sqrt{\frac{2}{3}}\gamma_{9},$$

$$G_{33} = -\frac{1}{3}\gamma_{7} + \frac{\sqrt{2}}{3}\gamma_{8} + \sqrt{\frac{2}{3}}\gamma_{9},$$
(A1)

in agreement with the Euclidean rotation of the Minkowskian version discussed in [22]. This representation can be related to that of [17] for d=4 Euclidean dimensions through a spin-base transformation. While (A1) can be constructed from 9 Euclidean Dirac matrices  $\gamma_{1,...,9}$ , a Euclidean construction satisfying also reflection positivity requires a nontrivial spin metric h for the definition of a Luttinger conjugate spinor  $\bar{\psi}=\psi^{\dagger}h$ . As detailed in [13, 22], this demands for an at least  $d_{\gamma}=32$  dimensional representation of the Euclidean Dirac algebra, going along with two further anti-commuting elements  $\gamma_{10}$  and  $\gamma_{11}$ . In the present work, we use  $\gamma_{10}$  for the construction of the spin metric,  $h=\gamma_1\gamma_2\gamma_3\gamma_{10}$ , while  $\gamma_{11}$  is employed for the definition of the Yukawa interaction of our model. Various other choices would alternatively be possible, cf. [22].



282

## Appendix B: Threshold Functions

The threshold functions used in the main text, are classified and defined for general regulator functions in the literature [30, 36, 37, 64, 65]. As the Luttinger fermions come with a new kinetic term, several new threshold functions are needed which can be defined in full analogy to those involving, for instance, Dirac fermions.

For the regulator, we choose in the scalar and the fermionic sectors

$$R_{k,\phi}(p^2) = Z_{\phi}p^2(1 + r_{\rm B}(p^2/k^2)),$$

$$R_{k,\psi}(p^2) = Z_{\psi}G_{\mu\nu}p^{\mu}p^{\nu}(1 + r_{\rm L}(p^2/k^2)),$$
(A2)

where  $r_{\rm B}(y)$ ,  $r_{\rm L}(y)$  denote dimensionless regulator shape functions that encode the momentum space regularization near  $p^2 \sim k^2$ . Introducing the following auxiliary functions related to the regularized momentum-space propagators

$$G_{\rm B}(\omega) = \frac{1}{y(1+r_{\rm B})+\omega}, G_{\rm L}(\omega) = \frac{1}{y^2(1+r_{\rm L})^2+\omega},$$
 (A3)

where  $y = p^2/k^2$ , the threshold functions involving Luttinger fermions occurring in the main text are defined by

$$l_0^{(\mathrm{L})d}(\omega;\eta) = \frac{k^{-d}}{4v_d} \int_p \tilde{\partial}_t \ln G_{\mathrm{L}}^{-1}(\omega), \tag{A4}$$

$$l_{1,1}^{(\text{LB}) d}(\omega_1, \omega_2; \eta_1, \eta_2) = \frac{k^{-d}}{4v_d} \int_p \tilde{\partial}_t G_{\mathcal{L}}(\omega_1) G_{\mathcal{B}}(\omega_2),$$
 (A5)

$$m_{1,2}^{(\text{LB}),d}(\omega_1,\omega_2;\eta_1,\eta_2) = -\frac{k^{-d}}{4v_d} \int_p dy \ y^2 \tilde{\partial}_t [(G_{\text{B}}(\omega_2))''(1+r_{\text{L}})G_{\text{L}}(\omega_1)], \tag{A6}$$

$$\begin{split} m_4^{(\mathrm{L}),d}(\omega,\eta) &= -\frac{k^{-d}}{4v_d} \int_p y \, \tilde{\partial}_t \bigg\{ \big[ (y(1+r_L)G_{\mathrm{L}}(\omega))' \big]^2 \\ &+ \frac{d}{2} (1+r_{\mathrm{L}})^2 G_{\mathrm{L}}^2(\omega) \bigg\}, \end{split} \tag{A7}$$

$$m_2^{(L),d}(\omega,\eta) = -\frac{k^{-d}}{4v_d} \int_{p} y \,\tilde{\partial}_t [(G_L(\omega))']^2,$$
 (A8)

where, in practice, the derivative  $\tilde{\partial}_t$  can be read as  $\tilde{\partial}_t \to (\partial_t r - \eta r)\partial_r$ ,  $\int_n \equiv \int \frac{d^d p}{(2\pi)^d}$  indicates the full momentum integral, and primes denote derivatives with respect to v.

For all concrete computations in the main text, we use the partially linear regulator (Litim regulator) [66, 67],



$$r_{\rm B} = r_{\rm L} = \left(\frac{1}{y} - 1\right)\theta(1 - y),\tag{A9}$$

which allows for an analytic evaluation of the loop momentum integration. The corresponding threshold functions then read

$$l_0^{(L)\,d}(\omega;\eta) = \frac{4}{d} \left( 1 - \frac{\eta}{d+2} \right) \frac{1}{1+\omega},$$
 (A10)

$$l_{1,1}^{(LB) d}(\omega_1, \omega_2; \eta_1, \eta_2) = \frac{2}{d} \frac{1}{(1 + \omega_1)(1 + \omega_2)} \times \left(\frac{2}{1 + \omega_1} \left(1 - \frac{\eta_1}{d + 2}\right) + \frac{1}{1 + \omega_2} \left(1 - \frac{\eta_2}{d + 2}\right)\right), \tag{A11}$$

$$m_{1,2}^{(\text{LB}),d}(\omega_1, \omega_2; \eta_1, \eta_2) = \frac{1}{2} \frac{1}{(1+\omega_1)(1+\omega_2)^2} \times \left(d+1 + \frac{\omega_1 - 3}{\omega_1 + 1} - \eta_2\right),$$
(A12)

$$m_4^{(L),d}(\omega,\eta) = \frac{(1-\omega)^2}{(1+\omega)^4} + \frac{2(d-\eta)}{d-2} \frac{1-\omega}{(1+\omega)^3},$$
(A13)

$$m_2^{(L),d}(\omega,\eta) = \frac{4}{(1+\omega)^4}.$$
 (A14)

For completeness, we also list all other required threshold functions known from the literature [30, 36, 37, 64, 65]:

$$l_0^d(\omega;\eta) = \frac{2}{d} \left( 1 - \frac{\eta}{d+2} \right) \frac{1}{1+\omega},\tag{A15}$$

$$m_{2,2}^d(\omega;\eta) = \frac{1}{(1+\omega)^4}.$$
 (A16)

Because of the nonanalyticity of the Litim regulator, the m-type threshold functions partly involve ill-defined products of distributions such as  $\delta(1-y)\theta(1-y)$ . This is a result of using the derivative expansion of the action as an ansatz; including full momentum-dependencies would lead to perfectly well-defined flows. In the present case, the problematic products occuring here can straightforwardly be cured by suitably smearing the singularity of the Heaviside function. Using a symmetric smearing, it can be shown that the resulting loop integrations can effectively be performed by the simple replacement  $\delta(1-y)\theta(1-y) \to \frac{1}{2}\delta(1-y)$ . This recipe is in agreement with the results used in the literature.



**Acknowledgements** We thank Lukas Janssen, David Moser, Michael Scherer, Richard Schmieden, and Christof Wetterich for valuable discussions. We are grateful to Richard Schmieden for his kind assistance with the numerical implementation and the code development. HG thanks the ITP Heidelberg for hospitality while working on this project. This work has been funded by the Deutsche Forschungsgemeinschaft (DFG) under Grant No. 406116891 within the Research Training Group RTG 2522/1.

Author Contributions Both authors have contributed equally.

Funding Open Access funding enabled and organized by Projekt DEAL.

**Data Availability** No datasets were generated or analysed during the current study.

#### **Declarations**

Competing interests The authors declare no competing interests.

**Open Access** This article is licensed under a Creative Commons Attribution 4.0 International License, which permits use, sharing, adaptation, distribution and reproduction in any medium or format, as long as you give appropriate credit to the original author(s) and the source, provide a link to the Creative Commons licence, and indicate if changes were made. The images or other third party material in this article are included in the article's Creative Commons licence, unless indicated otherwise in a credit line to the material. If material is not included in the article's Creative Commons licence and your intended use is not permitted by statutory regulation or exceeds the permitted use, you will need to obtain permission directly from the copyright holder. To view a copy of this licence, visit <a href="http://creativecommons.org/licenses/by/4.0/">http://creativecommons.org/licenses/by/4.0/</a>.

#### References

- Zinn-Justin, J.: Int. Ser. Monogr. Phys. 77, 1 (1989)
- 2. 't Hooft, G.: NATO Sci. Ser. B **59**,, 135 (1980)
- 3. Giudice, G.F.: 155 (2008). arXiv:0801.2562 [hep-ph]
- 4. Grinstein, B., O'Connell, D., Wise, M.B.: Phys. Rev. D 77, 025012 (2008). arXiv:0704.1845 [hep-ph]
- 5. Hossenfelder, S.: Synthese **198**, 3727 (2021). arXiv:1801.02176 [physics.hist-ph]
- 6. Bak, P., Tang, C., Wiesenfeld, K.: Phys. Rev. Lett. **59**, 381 (1987)
- 7. Bak, P., Tang, C., Wiesenfeld, K.: Phys. Rev. A 38, 364 (1988)
- 8. Manna, S.S.: J. Phys. A: Math. Gen. **24**, L363 (1991)
- 9. Olami, Z., Feder, H.J.S., Christensen, K.: Phys. Rev. Lett. 68, 1244 (1992)
- 10. Malamud, B.D., Morein, G., Turcotte, D.L.: Science 281, 1840 (1998)
- 11. Vespignani, A., Zapperi, S.: Phys. Rev. E 57, 6345–6362 (1998)
- 12. Bornholdt, S., Wetterich, C.: Phys. Lett. B 282, 399 (1992)
- Gies, H., Heinzel, P., Laufkötter, J., Picciau, M.: Phys. Rev. D 110, 065001 (2024). arXiv:2312.12058 [hep-th]
- 14. Luttinger, J.M.: Phys. Rev. 102, 1030 (1956)
- 15. Murakami, S., Nagosa, N., Zhang, S.-C.: Phys. Rev. B 69, 235206 (2004). arXiv:cond-mat/0310005
- Moon, E.-G., Xu, C., Kim, Y.B., Balents, L.: Phys. Rev. Lett. 111, 206401 (2013). arXiv:1212.1168 [condmat.str-el]
- 17. Janssen, L., Herbut, I.F.: Phys. Rev. B 92, 045117 (2015). arXiv:1503.04242 [cond-mat.str-el]
- 18. Janssen, L., Herbut, I.F.: Phys. Rev. B 95, 075101 (2017). arXiv:1611.04594 [cond-mat.str-el]
- 19. Ray, S., Vojta, M., Janssen, L.: Phys. Rev. B 98, 245128 (2018). arXiv:1810.07695 [cond-mat.str-el]
- 20. Dey, S., Maciejko, J.: Phys. Rev. B 106, 035140 (2022). arXiv:2204.05319 [cond-mat.str-el]
- Moser, D.J., Janssen, L.: Rep. Prog. Phys. 88 098001 (2025), [cond-mat.str-el] https://doi.org/10.1088/ 1361-6633/ae01d5
- 22. Gies, H., Picciau, M.: Phys. Rev. D 111, 085001 (2025). arXiv:2410.22166 [hep-th]
- 23. Abrikosov, A.A.: Sov. Phys. JETP 39, 709 (1974)



- 24. Holland, K., Kuti, J.: Lattice hadron physics. Proceedings, 2nd topical workshop, LHP 2003, Cairns, Australia, July 22-30, 2003, Nucl. Phys. Proc. Suppl. 129, 765 (2004), [,765(2003)], arXiv:heplat/0308020 [hep-lat]
- 25. Holland, K.: Lattice field theory. Proceedings, 22nd international symposium, Lattice 2004, Batavia, USA, June 21-26, 2004, Nucl. Phys. Proc. Suppl. 140, 155 (2005), [,155(2004)], arXiv:hep-lat/0409112 [hep-lat]
- 26. Branchina, V., Faivre, H.: Phys. Rev. D 72, 065017 (2005). arXiv:hep-th/0503188 [hep-th]
- 27. Branchina, V., Faivre, H., Pangon, V.: J. Phys. **G36**, 015006 (2009), arXiv:0802.4423 [hep-ph]
- 28. Gies, H., Gneiting, C., Sondenheimer, R.: Phys. Rev. D 89, 045012 (2014). arXiv:1308.5075 [hep-ph]
- 29. Wetterich, C.: Phys. Lett. B 301, 90 (1993)
- 30. Berges, J., Tetradis, N., Wetterich, C.: Phys. Rept. 363, 223 (2002). arXiv:hep-ph/0005122 [hep-ph]
- 31. Pawlowski, J.M.: Annals Phys. 322, 2831 (2007). arXiv:hep-th/0512261 [hep-th]
- Gies, H.: ECT\* School on renormalization group and effective field theory approaches to many-body systems trento, Italy, February 27-March 10, 2006, Lect. Notes Phys. 852, 287 (2012), arXiv:hep-ph/0611146 [hep-ph]
- 33. Delamotte, B.: Lect. Notes Phys. 852, 49 (2012). arXiv:cond-mat/0702365 [cond-mat.stat-mech]
- 34. Braun, J.: J. Phys. **G39**, 033001 (2012). arXiv:1108.4449 [hep-ph]
- 35. Dupuis, N., Canet, L., Eichhorn, A., Metzner, W., Pawlowski, J.M., Tissier, M., Wschebor, N.: Phys. Rept. 910, 1 (2021). arXiv:2006.04853 [cond-mat.stat-mech]
- 36. Jungnickel, D.U., Wetterich, C.: Phys. Rev. D 53, 5142 (1996). arXiv:hep-ph/9505267 [hep-ph]
- 37. Hofling, F., Nowak, C., Wetterich, C.: Phys. Rev. B 66, 205111 (2002). arXiv:cond-mat/0203588 [condmat]
- 38. Diehl, S., Floerchinger, S., Gies, H., Pawlowski, J.M., Wetterich, C.: Annalen Phys. 522, 615 (2010). arXiv:0907.2193 [cond-mat.quant-gas]
- 39. Braun, J., Gies, H., Scherer, D.D.: Phys. Rev. D 83, 085012 (2011). arXiv:1011.1456 [hep-th]
- 40. Mesterhazy, D., Berges, J., von Smekal, L.: Phys. Rev. B 86, 245431 (2012). arXiv:1207.4054 [condmat.str-el]
- 41. Jakovác, A., Patkòs, A., Pòsfay, P.: Eur. Phys. J. C 75, 2 (2015). arXiv:1406.3195 [hep-th]
- 42. Janssen, L., Herbut, I.F.: Phys. Rev. B 89, 205403 (2014), arXiv:1402.6277 [cond-mat.str-el]
- 43. Vacca, G.P., Zambelli, L.: Phys. Rev. D 91, 125003 (2015). arXiv:1503.09136 [hep-th]
- 44. Gies, H., Sondenheimer, R.: Eur. Phys. J. C 75, 68 (2015). arXiv:1407.8124 [hep-ph]
- 45. Classen, L., Herbut, I.F., Janssen, L., Scherer, M.M.: Phys. Rev. B 93, 125119 (2016). arXiv:1510.09003 [condmat.str-el]
- 46. Knorr, B.: Phys. Rev. B **94**, 245102 (2016). arXiv:1609.03824 [cond-mat.str-el]
- 47. Fu, W.J., Pawlowski, J.M., Rennecke, F., Schaefer, B.J.: Phys. Rev. D 94, 116020 (2016). arXiv:1608.04302 [hep-ph]
- 48. Stoll, J., Zorbach, N., Koenigstein, A., Steil, M.J., Rechenberger, S.: (2021), arXiv:2108.10616 [hep-ph]
- 49. Gies, H., Schmieden, R., Zambelli, L.: Eur. Phys. J. C 85, 56 (2025). arXiv:2306.05943 [hep-th]
- 50. Hawashin, B., Eichhorn, A., Janssen, L., Scherer, M.M., Ray, S.: Nature Commun. 16, 20 (2025). arXiv:2312.11614 [cond-mat.str-el]
- 51. Bervillier, C., Juttner, A., Litim, D.F.: Nucl. Phys. B 783, 213 (2007). arXiv:hep-th/0701172
- 52. Borchardt, J., Knorr, B.: Phys. Rev. D **91**, 105011 (2015). arXiv:1502.07511 [hep-th]
- 53. Borchardt, J., Knorr, B.: Phys. Rev. D **94**, 025027 (2016). arXiv:1603.06726 [hep-th]
- 54. Borchardt, J., Gies, H., Sondenheimer, R.: Eur. Phys. J. C 76, 472 (2016). arXiv:1603.05861 [hep-ph]
- 55. Grossi, E., Wink, N.: SciPost Phys. Core 6, 071 (2023). arXiv:1903.09503 [hep-th]
- 56. Koenigstein, A., Steil, M.J., Wink, N., Grossi, E., Braun, J., Buballa, M., Rischke, D.H.: Phys. Rev. D **106**, 065012 (2022). arXiv:2108.02504 [cond-mat.stat-mech]
- 57. Ihssen, F., Pawlowski, J.M., Sattler, F.R., Wink, N.: Comput. Phys. Commun. 300, 109182 (2024). arXiv:2207.12266 [hep-th]
- 58. Ihssen, F., Sattler, F.R., Wink, N.: Phys. Rev. D 107, 114009 (2023). arXiv:2302.04736 [hep-th]
- 59. Sattler, F.R., Pawlowski, J.M.: (2024), arXiv:2412.13043 [hep-ph]
- O'Raifeartaigh, L., Wipf, A., Yoneyama, H.: Nucl. Phys. B 271, 653 (1986)
- 61. Litim, D.F., Pawlowski, J.M., Vergara, L.: (2006), arXiv:hep-th/0602140 [hep-th]
- 62. Zorbach, N., Stoll, J., Braun, J.: (2024), arXiv:2401.12854 [hep-ph]
- 63. Zorbach, N., Koenigstein, A., Braun, J.: (2024), arXiv:2412.16053 [cond-mat.stat-mech]
- 64. Gies, H., Rechenberger, S., Scherer, M.M., Zambelli, L.: Eur. Phys. J. C 73, 2652 (2013). arXiv:1306.6508 [hep-th]
- 65. Gies, H., Ziebell, J.: Eur. Phys. J. C **80**, 607 (2020). arXiv:2005.07586 [hep-th]
- 66. Litim, D.F.: Phys. Lett. B **486**, 92 (2000). arXiv:hepth/0005245 [hep-th]
- 67. Litim, D.F.: Phys. Rev. D 64, 105007 (2001). arXiv:hepth/0103195 [hep-th]

Publisher's Note Springer Nature remains neutral with regard to jurisdictional claims in published maps and institutional affiliations.

